Dissipative soliton resonance and its depression into burst-like emission in a holmium-doped fiber laser with large normal dispersion

JUNQING ZHAO, [1] JIAN ZHOU, [1] LEI LI, [1] LUMING ZHAO, [1,2,*] DINGYUAN TANG, [1] DEYUAN SHEN, [1] AND LEI SU[2]

[1] *Jiangsu Key Laboratory of Advanced Laser Materials and Devices, Jiangsu Collaborative Innovation Center of Advanced Laser Technology and Emerging Industry, School of Physics and Electronic Engineering, Jiangsu Normal University, Xuzhou 221116, Jiangsu, China*
[2] *School of Engineering and Materials Science, Queen Mary University of London, London, UK*
**Corresponding author: lmzhao@ieee.org*

Received XX Month XXXX; revised XX Month, XXXX; accepted XX Month XXXX; posted XX Month XXXX (Doc. ID XXXXX); published XX Month XXXX

We report on dissipative soliton resonance (DSR) and its transformation into a type of burst-like emission in a holmium-doped fiber (HDF) laser in the large normal dispersion regime. A nonlinear amplifying loop mirror incorporating ~118 m large normal dispersion fiber acts as an artificial saturable absorber. The HDF laser has the largest net normal dispersion so far. As the pump power is increased from ~1.72 to ~4.80 W, the produced single pulse linearly broadens from ~6.7 to ~68.0 ns, whilst the output pulse peak power is clamped around ~180.5 mW due to the peak-power-clamping effect with the DSR. The sharp spectral peak indicates that the DSR is realized with a large normal dispersion. With further manipulation of the polarization state, the DSR can evolve into a type of burst-like emission. It is further revealed that this burst-like emission could be caused by a type of peak-power-depressing effect, which results from the competition between the DSR and soliton formation.

OCIS codes: *(140.3510) Lasers, fiber; (140.4050) Mode-locked lasers; (320.4240) Nanosecond phenomena.*

http://dx.doi.org/10.1364/OL.99.099999

Pulsed laser sources in 2 μm spectral region have attracted considerable attention in recent years due to their wide range of applications, such as mid-infrared coherent source, lidar, spectroscopy, and various materials processing. Thulium and holmium doped fiber laser sources have also increasingly stood out from conventional bulk systems due to their merits of excellent beam quality, high average power availability, compactness, flexibility, etc. Typically, the most efficient emission of thulium doped fiber (TDF) laser sources is within the 1.9-2 μm spectral region, although some attempts have been done to extend it (the lasing efficiency is still low for a too short or too long wavelength). Meanwhile, for longer-wavelength lasing holmium-doped fiber (HDF) provides an excellent choice, approaching the long wavelength limit of silica fibers [1].

To obtain a pulsed source using HDF, however, no efficient laser diodes (LDs) are available and, thus, a resonant pumping around 1.95 μm is typically used. Besides the limited pump selection, several other factors also exert challenges on the development of fiber sources beyond 2 μm. These include the large attenuation loss as approaching the wing of a vibrational absorption band of silica [1], the unavailability of particular fibers or components, the high-cost or even shortage of measurement equipment, etc.

Restricted by these factors, only several limited types of optical pulses have ever been demonstrated in passively mode-locked HDF lasers up to now, including typical solitons in all anomalous dispersion regime [2, 3], dispersion-managed solitons with a dispersion close to zero [4, 5], etc. Nevertheless, in view of the rich nonlinear dynamics of mode locked fiber lasers, other types of pulses should still be possible to be formed in HDF lasers.

Among the various mode-locked laser operations, recent years, particular attention has been paid to dissipative soliton resonance (DSR) due to its unparalleled potential in pulse energy scaling [6-9]. A DSR pulse is mainly shaped by an effect named as peak-power-clamping (PPC), which maintains the pulse peak power at a constant level during energy scaling. Although the DSR operation of many fiber lasers has been extensively studied, so far there is only one report on the DSR-like mode-locking in HDF lasers [10].

In this Letter, we demonstrate the first DSR operation in a large normal dispersion HDF laser at 2.05 μm. Furthermore, for the very first time, we observe the burst-like emission, as well as its related depression effect with the pulse peak power.

The configuration of the HDF laser is schematically illustrated in Fig. 1. A cascaded-pumping scheme is adopted to simplify the overall design. As shown, the pump for a piece of ~1.5 m long TDF is provided by a master oscillator power amplifier (MOPA) fiber

source seeded by a distributed feedback LD (DFB-LD) at ~1570.4 nm and power-boosted by a cladding-pumped erbium-ytterbium fiber amplifier (EYFA). The TDF has a small signal absorption coefficient at the pump wavelength of ~60 dB/m. The pump light is coupled into the TDF through a filter wavelength division multiplexer (FWDM), whose insertion losses around the 1570 nm pump and 2050 nm signal wavelengths are specified as ~0.39 and ~0.48 dB, respectively. This results a peak emission at ~1854 nm. It is subsequently used to intra-cavity resonant-pump a piece of HDF with length of ~2.1 m and small signal absorption at ~1854 nm of ~20 dB/m, respectively. A three-paddle fiber polarization controller (FPC), noted as FPC-1, is incorporated for polarization state (PS) adjustment. The fiber wrapped in it is a type of normal dispersion fiber (NDF, UHNA7, Nufern, Co.). The NDF exhibits a high numerical aperture of 0.41, a small core diameter of 2.4 μm, and a group velocity dispersion (GVD) of ~49.4 ps^2 /km at 2.05 μm [11]. The total used NDF length is ~118 m, resulting in a net cavity dispersion of ~4.9 ps^2, the largest normal dispersion so far for fiber lasers with emission beyond 2 μm. All other fibers as used are standard SMF-28e. Further employing a 3-dB fiber optical coupler (FOC), a nonlinear amplifying loop mirror (NALM) is constructed.

On the other side of the 3-dB FOC, a unidirectional propagation loop is constructed by incorporating an isolator. Within it, the second FPC, i.e., FPC-2, is used to manipulate the intra-cavity PS in combination with the FPC-1. A 20/80 FOC is used to extract ~20% optical power as the output. The total cavity length is ~128 m.

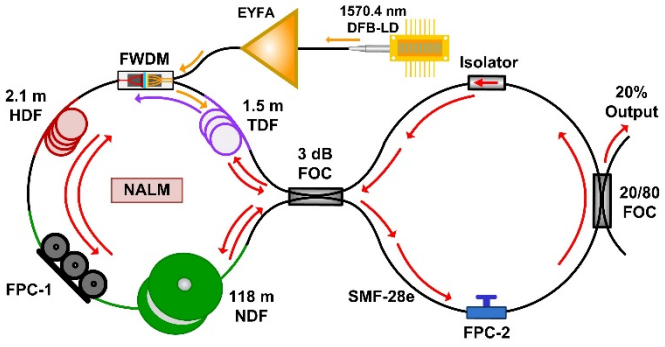

Fig. 1. Experimental configuration.

Continuous wave lasing at ~2.05 μm started with ~1.22 W pump power at ~1570.4 nm. Further increasing the pump power to ~1.72 W, stable single DSR pulse was produced by adjusting the two FPCs to appropriate orientations. Figure 2(a) 3D-plots several single pulse envelops as the pump power increased from ~1.72 to ~4.80 W. Meanwhile, the pulse duration scaled with the pump power in a roughly linear manner, from ~6.7 to ~68.0 ns, with a nearly fixed pulse peak power of ~180.5 mW, the well-known PPC effect, which is a signature characteristic of DSR pulse. The corresponding radio frequency (RF) traces were plotted as in Fig. 2(b), all with the same span of 0-100 MHz and resolution BW (RBW) of 1 kHz. Despite the cavity-determined sharp RF lines, a damped modulating behavior could be clearly noticed on each trace. The modulation frequency and the native pulse duration always satisfied a reciprocal relationship. All the temporal traces through this Letter were measured by using an extended InGaAs photodetector (ET-5000, Electro-Optics Technology, Inc.) with specified rise time/fall time of 28 ps/28 ps and bandwidth (BW) of >12.5 GHz, in combination with a digital oscilloscope (DSO9104A, Agilent Technologies, Inc.). Similarly, all the RF traces were detected by using the same photodetector and recorded with an RF spectrum analyzer (N9320B, Agilent Technologies, Inc.).

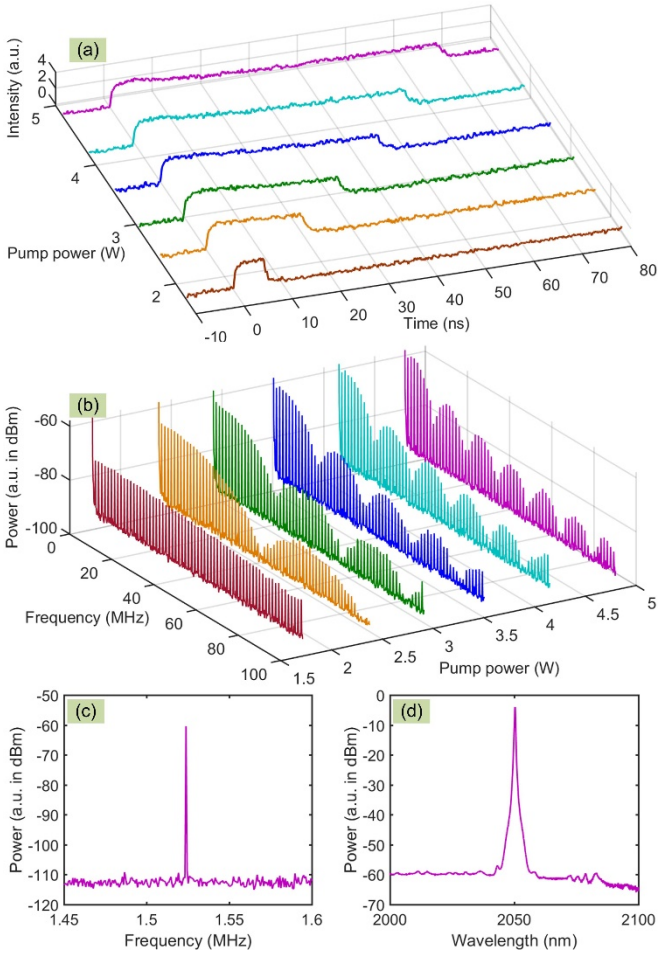

Fig. 2. Evolutions of (a) single DSR pulse and (b) the corresponding RF train with respect to pump power, respectively; (c) detailed RF around the PRF and (d) optical spectrum with pump power of ~4.80 W.

Figure 2(c) plotted a detailed RF spectrum (10 Hz RBW) around the pulse repetition frequency (PRF) with ~4.80 W pump power. It peaked at ~1.524 MHz and had a signal to noise ratio (SNR) of ~49 dB. The SNR rose from ~36 to ~49 dB as the pump power increasing from ~1.72 to ~4.80 W.

The output optical spectra were measured by using an optical spectrum analyzer (AQ6375B, Yokogawa Test & Measurement Co., Japan) with 0.05 nm resolution. Figure 2(d) plots a typical optical spectral profile pumped at ~4.80 W. it peaked at ~2050.373 nm with a 3-dB BW of ~0.378 nm. The narrow spectrum is a distinguished characteristic for a DSR with a normal dispersion.

By adjusting the two FPCs, we observed a type of burst-like emission as shown in Fig. 3, where the DSR pulse broke into a packet of many random pulses. Figure 3(a) plots a DSR pulse

envelop when the pump power was ~2.5 W. A burst-like state with the same pump power but a different PS is shown in Fig. 3(b). The duration of the packet with an identical condition was stable, but the internal pulses varied randomly. It was also noted that as the DSR pulse transferred into the burst-like emission, the packet widened from ~17.1 to ~85.4 ns. A burst-like emission trace with 10 μs span was captured in Fig. 3(c). As seen, the overall pulse packet repeated at the cavity roundtrip, despite the internal randomness. Figure 3(d) plots a detailed burst-like packet in a train. In the same train, the burst-like packet produced in the next roundtrip was shown in Fig. 3(e). Even with so short a time interval it could be seen that the internal pulses exhibited varied peak intensities. It means that there might be some competitions among the internal pulses, resulting in the random characteristics within each pulse packet.

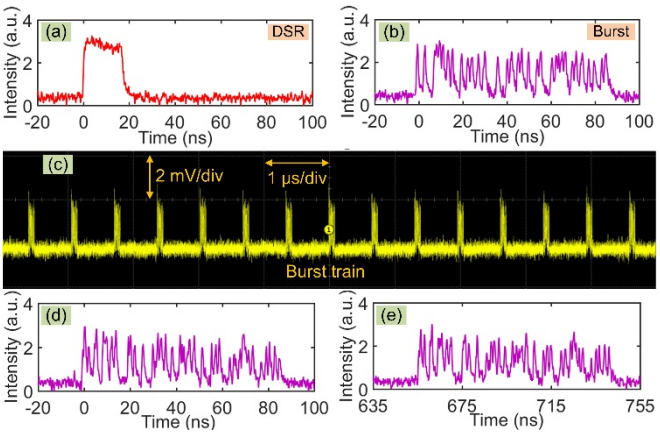

Fig. 3. (a) A DSR pulse envelop and (b) its transformation into a burst-like emission; (c) a typical trace with 10 μs span; (d) a burst-like packet in a train; (e) the next burst-like packet in the same train.

Further detailed observation revealed that the evolution from the DSR to burst-like emission could be seen as a type of peak-power-depressing (PPD) process. For comparison, Fig. 4(a) plots a typical pulse envelop when the HDF laser was operating with the DSR at ~4.8 W pump power. The corresponding intra-cavity PS was noted as PS1. Tuning the PS to a noted PS2, we observed two sharp depressions on the pulse envelop [Fig. 4(b)]. Further tuning to a noted PS3, more and stronger depressions appeared [Fig 4(c)]. Finally, a burst-like emission state containing a great number of internal pulses formed at a noted PS4, seen in Fig. 4(d).

As displayed in Fig. 4, as more depressions appeared along the packet profile, the packet duration became longer. The initial DSR pulse duration was ~68.0 ns, and the final burst-like packet duration increased to ~139.0 ns. We believe that the depressions were caused by pulse breaking during polarization modulations. The existence of anomalous dispersion fiber segment facilitated the pulse breaking .

Figure 4(e) plots a typical optical spectrum of the burst-like emission when the pump power was ~4.80 W, corresponding to the temporal trace in Fig. 4(d). Compared to the optical spectrum of the DSR pulse in Fig. 2(d), here one significant difference is that several sharp spikes appeared on the spectral profile. Another difference was that the main spectral peak broadened and shifted from ~2050.373 to ~2046.940 nm. Adjustment of the FPCs varied the local fiber birefringence, which then altered the transmittance of the NALM as well as the overall effective laser gain, including the effective gain profile and gain location. This consequently resulted in the change of the detailed spectral profile and even the shift of the spectral peak. Once the burst-like pulses were obtained, pump power increasing made the burst-like packet broadened, together with output power increasing. Under the same pump power, the output power of burst-like pulses is larger than that of DSR pulses.

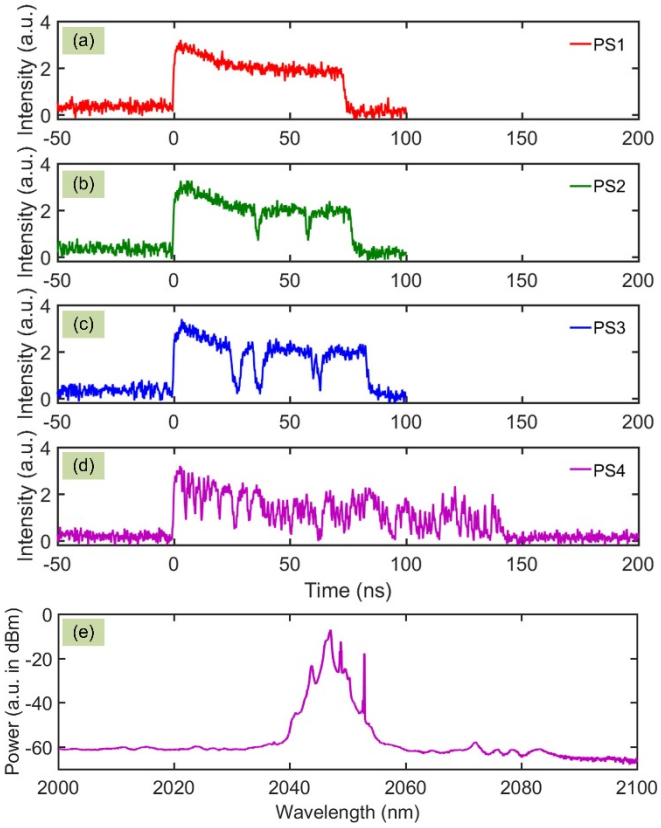

Fig. 4. (a)-(d) Depressing process from DSR to burst-like emission; (e) typical output optical spectrum of the burst-like emission.

The developing process from a DSR pulse to the burst-like emission is repeatable. However, it is a one-way process and the DSR pulse should be achieved first. Generally, if we want to get back to the same DSR pulse profile, we have to achieve it first, and then we can further get a similar evolving process from the DSR to the burst-like emission. However, the newly obtained burst-like emission are typically different from the one obtained last time due to the random characteristics within the pulse package.

The appearance of Kelly-sideband-similar structure [12] indicates that the internal pulses are evolving towards solitons. This is possible considering that the used HDF, TDF, and SMF-28e are all with anomalous dispersion around ~2.05 μm, although their total dispersion is small compared with that of the used NDF. Thus, there is still some possibility that the locally anomalous dispersion effect can dominate the pulse shaping [13], especially when the polarization modulation is on-going. The formed solitons

would repel each other, resulting in a temporally stable multi-pulse state if no other mechanisms packing them together. However, due to the strong PPC effect, the formed solitons could not completely split from each other, equivalent to an effective attraction that imposed a limitation on the achievable packet duration. The evolving towards solitons and the packet-duration limitation resulted in the burst-like emission. The emission states in Figs. 4(a), 4(b), and 4(c) are some intermediate cases as the DSR pulse evolving into a burst of solitons. The PPC effect always plays its role to limit pulse peak power no matter it is a DSR pulse or a burst of solitons. Consequently, the DSR pulse and the burst-like pulses have a similar amplitude.

We noted that the DSR pulse and burst-like pulses were realized with different polarization settings. The optical spectrum of the DSR pulse [Fig. 2(d)] was clearly different from that of burst-like pulses [Fig. 4(e)]. Experimentally, we attempted to check whether the generated DSR pulse is a perfect pulse without internal structure. However, due to the nanosecond pulse duration and the narrow spectrum, the traditional pulse compression was difficult to be carried out. Autocorrelation measurement showed no internal structure in the DSR pulse. No matter how we changed the operation conditions while maintaining the DSR pulse generation, neither spectral modulation/dip corresponding to stable tightly packaged solitons or blurred optical spectrum corresponding a bunch with moving solitons [14] could be observed. Therefore, it is sufficient to claim that it is a DSR pulse rather than anything else.

Theoretically, DSR pulse could be generated in both normal dispersion regime and anomalous dispersion regime. However, experimentally we found that DSR pulse with narrow spectrum could be generated in normal dispersion regime (this paper) while the DSR-like pulse with broad spectrum could be generated in anomalous dispersion regime [10]. This is one of the most significant dispersion-induced effects on DSR. For DSR pulses short down to picosecond range the dispersion could also exert considerable effects on the duration.

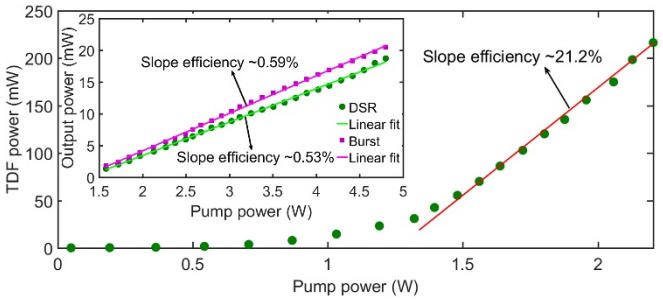

Fig. 5. Output power from the TDF pumped at 1570.4 nm. Inset: Average output power with the DSR and burst-like emission.

We have also measured the output power characteristics from the TDF pumped at 1570.4 nm, as depicted in Fig. 5. As seen once a threshold-like value of ~1.32 W was reached, a linear evolution could be achieved, giving a slope efficiency of ~21.2%. The inset further plots the average output power of both the DSR and burst-like emission characteristics against the ~1570.4 nm pump power. The average output power and slope efficiency were slightly higher when the laser is operated with the burst-like emission than that with the DSR, probably due to the PS-related different effective gains. The low slope efficiencies are mainly resulted from the two-step conversions with the utilized cascaded-pumping scheme: from ~1570 to ~1854 nm then from ~1854 to ~2050 nm.

In conclusion, we have experimentally realized the DSR operation in an HDF laser with large normal cavity dispersion and observed its depression into a burst-like emission, for the first time. Our results show new features of the DSR mode-locked pulses in the HDF laser, which enrich the dynamics of passively mode-locked fiber lasers.

Funding. National Natural Science Foundation of China (NSFC) (61705094, 11911530083, 11674133, 61575089), Natural Science Foundation of Jiangsu Province (BK20170243), Royal Society (IE161214); Natural Science Foundation of the Higher Education Institutions of Jiangsu Province (18KJB180004); Protocol of the 37th Session of China-Poland Scientific and Technological Cooperation Committee (37-17); European Union's Horizon 2020 research and innovation programme under the Marie Skłodowska-Curie grant agreement No. 790666.

Acknowledgment. We acknowledge Jiangsu Overseas Visiting Scholar Program for University Prominent Young & Middle-aged Techers and Presidents; Priority Academic Program Development of Jiangsu Higher Education Institutions (PAPD).

References

1. A. S. Kurkov, E. M. Sholokhov, V. B. Tsvetkov, A. V. Marakulin, L. A. Minashina, O. I. Medvedkov, and A. F. Kosolapov, Quantum Electron. **41**, 492 (2011).
2. A. Chamorovskiy, A. V. Marakulin, S. Ranta, M. Tavast, J. Rautiainen, T. Leinonen, A. S. Kurkov, and O. G. Okhotnikov, Opt. Lett **37**, 1448 (2012).
3. A. Y. Chamorovskiy, A. V. Marakulin, A. S. Kurkov, and O. G. Okhotnikov, Laser Phys. Lett. **9**, 602 (2012).
4. P. Li, A. Ruehl, U. Grosse-Wortmann, and I. Hartl, Opt. Lett. **39**, 6859 (2014).
5. M. Pawliszewska, T. Martynkien, A. Przewłoka, and J. Sotor, Opt. Lett. **43**, 38 (2018).
6. W. Chang, A. Ankiewicz, J. M. Soto-Crespo, and N. Akhmediev, Phys. Rev. A **78**, 023830 (2008).
7. J. Zhao, D. Ouyang, Z. Zheng, M. Liu, X. Ren, C. Li, S. Ruan, and W. Xie, Opt. Express **24**, 12072 (2016).
8. G. Semaan, F. B. Braham, J. Fourmont, M. Salhi, F. Bahloul, and F. Sanchez, Opt. Lett. **41**, 4767 (2016).
9. L. Zhao , D. Li, L. Li, X. Wang, Y. Geng, D. Shen, and L. Su, IEEE J. Sel. Topics Quantum Electron. **24**, 8800409 (2018).
10. J. Zhao , L. Li, L. Zhao , D. Tang, and D. Shen, IEEE Photon. Technol. Lett. **30**, 1699 (2018).
11. P. Ciąćka, A. Rampur, A. Heidt, T. Feurer, and M. Klimczak, J. Opt. Soc. Am. B **35**, 1301 (2018).
12. S. M. J. Kelly, Electron. Lett. **28**, 806 (1992).
13. X. Wu, D. Y. Tang, L. M. Zhao, and H. Zhang, Phys. Rev. A **80**, 013804 (2009).
14. L. M. Zhao, D. Y. Tang, H. Zhang, X. Wu, Opt. Express, **17**, 8103 (2009).

Detailed References

1. Andrei S. Kurkov, E. M. Sholokhov, V. B. Tsvetkov, A. V. Marakulin, L. A. Minashina, O. I. Medvedkov, and A. F. Kosolapov, "Holmium fibre laser with record quantum efficiency," Quantum Electron. **41**(6), 492-494 (2011). https://doi.org/10.1070/QE2011v041n06ABEH014565
2. A. Chamorovskiy, A. V. Marakulin, S. Ranta, M. Tavast, J. Rautiainen, T. Leinonen, A. S. Kurkov, and O. G. Okhotnikov, "Femtosecond mode-locked holmium fiber laser pumped by semiconductor disk laser," Opt. Lett **37**(9), 1448-1450 (2012). https://doi.org/10.1364/OL.37.001448
3. A. Y. Chamorovskiy, A. V. Marakulin, A. S. Kurkov, and O. G. Okhotnikov, "Tunable Ho-doped soliton fiber laser mode-locked by carbon nanotube saturable absorber," Laser Phys. Lett. 9(8), 602-606 (2012). https://doi.org/10.7452/lapl.201210094
4. Peng Li, Axel Ruehl, Uwe Grosse-Wortmann, and Ingmar Hartl, "Sub-100 fs passively mode-locked holmium-doped fiber oscillator operating at 2.06 μm," Opt. Lett. **39** (24), 6859-6862 (2014). https://doi.org/10.1364/OL.39.006859
5. Maria Pawliszewska, Tadeusz Martynkien, Aleksandra Przewłoka, and Jarosław Sotor, "Dispersion-managed Ho-doped fiber laser mode-locked with a graphene saturable absorber," Opt. Lett. **43** (1), 38-41 (2018) https://doi.org/10.1364/OL.43.000038
6. W. Chang, A. Ankiewicz, J. M. Soto-Crespo, and N. Akhmediev, "Dissipative soliton resonances," Phys. Rev. A **78**(2), 023830 (2008). https://doi.org/10.1103/PhysRevA.78.023830
7. Junqing Zhao, Deqin Ouyang, Zhijian Zheng, Minqiu Liu, Xikui Ren, Chunbo Li, Shuangchen Ruan, and Weixin Xie, "100 W dissipative soliton resonances from a thulium-doped double-clad all-fiber-format MOPA system," Opt. Express **24** (11), 12072-12081 (2016). https://doi.org/10.1364/OE.24.012072
8. Georges Semaan, Fatma Ben Braham, Jorel Fourmont, Mohamed Salhi, Faouzi Bahloul, and François Sanchez, "10 μJ dissipative soliton resonance square pulse in a dual amplifier figure-of-eight double-clad Er:Yb mode-locked fiber laser," Opt. Lett. **41** (20), 4767-4770 (2016). https://doi.org/10.1364/OL.41.004767
9. Luming Zhao , Daojing Li, Lei Li, Xuan Wang, Ying Geng, Deyuan Shen, and Lei Su, "Route to Larger Pulse Energy in Ultrafast Fiber Lasers," IEEE J. Sel. Topics Quantum Electron. **24** (3), 8800409 (2018). 10.1109/JSTQE.2017.2771739
10. Junqing Zhao , Lei Li, Luming Zhao , Dingyuan Tang, and Deyuan Shen, "Dissipative Soliton Resonances in a Mode-Locked Holmium-Doped Fiber Laser," IEEE Photon. Technol. Lett. **30** (19), 1699 – 1702 (2018). 10.1109/LPT.2018.2866225
11. Piotr Ciąćka, Anupamaa Rampur, Alexander Heidt, Thomas Feurer, and Mariusz Klimczak, "Dispersion measurement of ultra-high numerical aperture fibers covering thulium, holmium, and erbium emission wavelengths," J. Opt. Soc. Am. B **35** (6), 1301-1307 (2018). https://doi.org/10.1364/JOSAB.35.001301
12. S. M. J. Kelly, "Characteristic sideband instability of periodically amplified average soliton," Electron. Lett. **28** (8), 806-807 (1992). 10.1049/el:19920508
13. X. Wu, D. Y. Tang, L. M. Zhao, and H. Zhang, "Effective cavity dispersion shift induced by nonlinearity in a fiber laser," Phys. Rev. A **80** (1), 013804 (2009). https://doi.org/10.1103/PhysRevA.80.013804
14. L. M. Zhao, D. Y. Tang, H. Zhang, X. Wu, "Bunch of restless vector solitons in a fiber laser with SESAM," Optics Express, 17, 8103-8108 (2009). https://doi.org/10.1364/OE.17.008103